Experimental and numerical analysis of convective flow in a square cavity with internal protuberances

A Lizardi,[1] **H Terres, R López, M Vaca, S Chávez., A Lara, J R Morales**
Universidad Autónoma Metropolitana-Azcapotzalco, Departamento de Energía, Área de Termofluidos. Av. San Pablo 180, Col. Reynosa Tamaulipas, Del. Azcapotzalco, Ciudad de México.

E-mail: arlr@azc.uam.mx

Abstract. A comparison between experimental and numerical results for natural convection flow generated inside a square cavity filled with water, which has internal protuberances, is presented. The cavity is formed by vertical-isothermal and horizontal-adiabatic walls. The built prototype is integrated by: a clear glass square cavity, where internal protuberances are located; a cavity with water which maintains one of its walls at low temperature; an electrical resistance which preserves another wall at high temperature; and an array of mirrors. The experimental flow development was studied with a Particle Image Velocimetry (PIV) device. Furthermore, ANSYS software was used and mass, momentum and energy equations were numerically solved. Results were compared using a system with rectangular, semi-circular, and triangular protuberances versus a system without protuberances; it was found that: a) the maximum positive value of the vertical velocity decreased 7.12, 3.33 and 3.03%, respectively, for the experimental case, and 4.52, 2.26 and 1.27%, respectively, for the numerical case; b) the maximum positive value of the horizontal velocity decreased 18.37, 11.89 and 4.59%, respectively, for the experimental case, and 6.46, 4.75 and 2.47%, respectively, for the numerical case; c) the average Nusselt number decreased 10.52, 7.95 and 6.06%, respectively, for the experimental case, and 12.01, 9.06 and 3.02%, respectively, for the numerical case.

1. Introduction

In natural convection fluid movement results from buoyancy forces imposed on the fluid when its density in the vicinity of the heat transfer surface decreases or increases as a result of warming or cooling processes. Natural convection is a process of energy transport by the combined action of heat conduction, energy storage, and movement of matter. The complexity of the majority of the cases involving the transfer of heat by natural convection makes it impossible to have an exact analysis of the equations of conservation, having to resort to numerical simulations or experiments. The objective of this study is to compare the experimental and numerical results of the flow field in a square cavity filled with water, in four cases: without internal protuberances, and with internal rectangular, semi-circular and triangular protuberances, located symmetrically on the lower part of the system, as illustrated in Figure 1. The experimental analysis is accomplished by building a model that consists of: a square cavity of transparent glass that houses the internal protuberances under study; a cavity with water that maintains one of its walls at low temperature; an electric heater that keeps its wall at high temperature; and an arrangement of mirrors to aid light reflection. The experimental development of

[1] To whom any correspondence should be addressed.

the flow is done with a Velocimetry by Images of Particles device (PIV). Regarding, numerical solution, the equations of conservation of mass, momentum and energy are solved for permanent, two-dimensional, flow, together with the boundary conditions, using the finite element numerical method, by means of the ANSYS software.

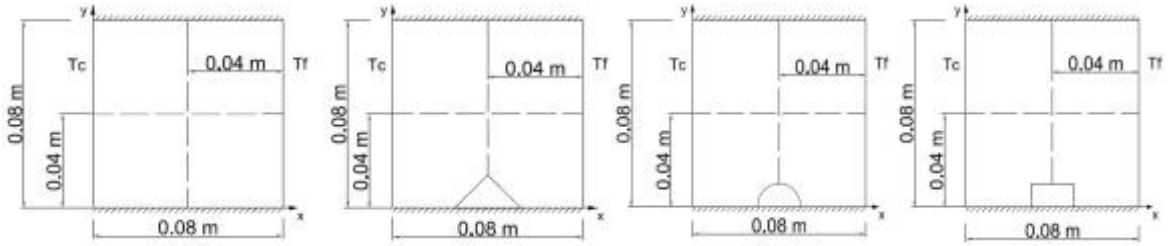

Figure 1. Physical representation of the problem and reference axes (dashed lines) for the analysis.

From the experimental point of view, the phenomenon of natural convection in cavities has been studied by various researchers. Some studies relating to this work are: Corvaro and Paroncini [1], experimentally analysed the natural convection in a square cavity full of air, with a rectangular fountain located at the bottom. The structure of the flow was analyzed for different numbers of Rayleigh and different positions of power source. The experimental apparatus used was a 2D-PIV, which determined the fields of streamlines and velocity maps. Corvaro et al. [2], experimentally analyzed the natural convection in a square cavity filled with air at atmospheric pressure using a PIV and holographic interferometry. Two (hot and cold) plates on the vertical sides of the box were placed. They investigated the relationship between the dynamic and temperature fields to describe how the flow and transfer of heat in the interior of the cavity were influenced by the temperature of the hot plate and the position of the cold plate. Nardini and Paroncini. [3], analyzed the effects on natural convection caused by the variation of the dimensions and positions of heat sources on the side walls of a square cavity filled with air. Temperature distributions were obtained, heat transfer coefficients were experimentally measured, using the holographic interferometry technique and compared to numerical results. On the other hand, reports relating to this topic, but from the numerical point of view are: Kaviany [4], numerically analyzed temperature fields and streamlines in a square cavity filled with air, with a semi-circular protuberance. The vertical walls were considered at constant temperature. The top and bottom surfaces were treated as adiabatic. Results of the number of Nusselt and maximum values of the stream function for a range of $10^1<Ra<10^4$ Rayleigh number and radii of the protuberance of 0, 0.2, and 0.4, are presented. Qi-Hong [5], numerically analyzed natural convection in a square cavity filled with air with two or three pairs of sources of heat in the vertical side walls. The analysis focuses on the effects of size and arrangement of sources and sinks on flow and heat transfer characteristics. Wang and Pepper [6], analyzed laminar natural convection in vertical channels with obstructions inside the channels. The results illustrate the temperature fields and streamlines for different parameters (number of Rayleigh, geometric relationship and location of obstructions) for smooth and blocked channels.

2. Experimental apparatus

In order to determine the properties of the flow in a square cavity inside with protuberances on the inside, we designed and built a test bench consisting of the following elements (Figure 2 - 3):

- A model, built in 0.006 m-thick glass, 0.4 m long, 0.22 m in height and 0.05 m in width. The model contains in itself: a system of mirrors which lights up the inside of the cavity and prevents the generation of shadows; a water tank of 0.14x0.1x0.05 m with an aluminum wall that provides the low temperature of the system; a 300 W electrical resistance mounted on an aluminum plate that provides the high temperature of the system; and a cavity of 0.08x0.1x0.05 m, which is the area of study. The protuberances were built in black-painted PVC to avoid light reflections. The rectangular protuberance

is 0.02 m base by 0.01 m in height, semi-circular protuberance has 0.010 m radius, and triangular protuberance is 0.028 m base by 0.014 m height.

- An electrical resistance of 300 W in the form of rectangular plate of 0.05x0.10 m.
- A voltage regulator of 120 V input, 0-140 V output and 10 A.
- A 380801 model EXTECH power Analyzer, with 0-300 W ±0.1 W, 0-200 V ±0.1 V and 0-2 A ±0.001A ranges.
- Eight type K thermocouples with a temperature range from -200°C to +1372ºC with a sensitivity of 41 μV/°C. Four thermocouples are placed inside the cavity, on the low-temperature aluminum plate with four others on the high-temperature aluminum plate with high temperature.
- A computer with the 8.1 Lab-View software installed. In this case, the program that allows the acquisition of data from eight thermocouples was previously prepared.
- A Dantec Dynamics Velocimetry by Images of Particles (VIP) apparatus.

Figure 2. Equipment calibration.

Figure 3. Velocimetry equipment and model.

3. Experimental procedure

Prior to experimentation, electrical resistance was calibrated with the power analyzer, finding that when the voltage regulator was operated at 20%, the electrical power was 50 W. This power was managed in all the experiments. The temperatures of the thermocouples were measured in steady state, from the hot and cold plates, being these of 22.3 and 19.3 °C, respectively. To determine the Nusselt number the temperature in the vicinity of the hot wall was determined by placing eight thermocouples along its vertical distance. The time that the equipment took achieve steady state was 10 minutes. Once these parameters were determined, the methodology described in Lizardi et al. [7] was used.

4. Mathematical formulations

The physical model consists of an enclosure of height and width H, the left vertical wall is at a high temperature Tc and the right temperature, at a low temperature Tf. The upper and lower walls are thermally insulated. Four settings were handled: cavity without protuberances on the inside and with rectangular, semi-circular and triangular protuberance in the background, as illustrated in Figure 1. The cavity was full of an incompressible Newtonian fluid, with constant physical properties, except for density in the term of buoyancy (Boussinesq approximation). Under these conditions, the density is considered as a linear function of the temperature, $\rho = \rho_o \left[1 - \beta \left(T - T_o\right)\right]$, Incropera and DeWitt [8]. The mathematical approach to the problem of flow promoted by natural convection is defined by the equations of continuity (1), quantity of movement in the x and y axis (2) and energy (3). The approximation of Boussinesq that considers the physical properties of the fluid to be independent of temperature is used in this study, Bejan [9]

$$\frac{\partial u}{\partial x} + \frac{\partial v}{\partial y} = 0 \tag{1}$$

$$\rho_o \left(u \frac{\partial u}{\partial x} + v \frac{\partial u}{\partial y} \right) = - \frac{\partial P}{\partial x} + \mu \left(\frac{\partial^2 u}{\partial x^2} + \frac{\partial^2 u}{\partial y^2} \right), \qquad \rho_o \left(u \frac{\partial v}{\partial x} + v \frac{\partial v}{\partial y} \right) = - \frac{\partial P}{\partial y} + \rho_o \, g \, \beta \, (T - T_o) + \mu \left(\frac{\partial^2 v}{\partial x^2} + \frac{\partial^2 v}{\partial y^2} \right) \tag{2}$$

$$\rho_o C\left(u\frac{\partial T}{\partial x}+v\frac{\partial T}{\partial y}\right)=k\left(\frac{\partial^2 T}{\partial x^2}+\frac{\partial^2 T}{\partial y^2}\right) \quad (3)$$

Appropriate boundary conditions for the system, Figure 1, are

x=0, u=v=0, T=Tc; x=H, u=v=0, T=Tf; y=0, u=v=0; y=H, u=v=0 (4)

5. Numerical treatment

To solve the equations of motion governing inside of system (1), (2) and (3), together with the boundary conditions (4), the method of the ANSYS finite element software was used. The following methodology was used, Moaveni and Saeed [10]:

a) The analysis, in this case FLOTRAN type is selected in the software.

b) The geometry to be analyzed is drawn, and elements in the boundaries are generated. In this case the cavity was dimensioned with a height and width of 0.08 m. The generation of nodes and elements was as follows: in the system without protuberance 3364 nodes with 6498 elements; in the rectangular protuberance 3428 nodes with 6604 elements; in the semi-circular protuberance 3449 nodes with 6664 elements; and in the triangular protuberance 3372 nodes with 6512 elements.

c) The value of the properties of the fluid, in this case water, which remain constant: dynamic viscosity, specific heat and thermal conductivity, volumetric expansion coefficient was fed. The density was handled as variable and pressure was modeled with the algorithm of relaxation (TDMA).

d) Boundary conditions were inserted and the software, was programmed for a maximum of 500 iterations. The foregoing was sufficient to reach the convergence of the problem.

It is worth mentioning that when the values of the thermophysical properties of water and the conditions of the cavities were fed, we obtained numbers of Prandtl of 6.87 and Rayleigh $2.705\text{x}10^6$.

6. Results and discussion

The experimental and numerical results of the fields of velocity, in m/s, are respectively presented in Figures 4-11. It can be observed that in the vicinity of the walls with high and low temperature fluid moves vertically towards the top and bottom boundary, respectively. In upper and lower adiabatic walls movement of the fluid is to the right and left, respectively. The combination of these flows generates a rotary motion in a clockwise direction. In Figure 12 the numerical and experimental results of vertical velocity, in m/s, for different positions in the x-axis and a location on the shaft "y" of 0.04 m, can be observed. For the non-protuberance system, the component of velocity starts out at zero. Following it can be observed that the flow of the hydrodynamic boundary layer is directed vertically toward the upper border. It can be seen that the magnitude of the vertical velocity increases up to a maximum of $6.60\text{x}10^{-4}$ and $7.07\text{x}10^{-4}$ m/s, respectively, and from there it begins to decrease to a value close to zero. From this point there are small fluctuations of the component of velocity along the central part of the system. Finally, the area of the other hydrodynamic boundary layer where now the flow is directed toward the lower border is observed. In this part the vertical velocity increases up to a maximum negative of $-6.83\text{x}10^{-4}$ and $-6.99\text{x}10^{-4}$ m/s, respectively, and from there again its magnitude decreases until it reaches zero. The same behavior is observed for the systems with rectangular, semi-circular, and triangular protuberance but with different values, in this case the maximum positive magnitudes are $6.13\text{x}10^{-4}$ and $6.75\text{x}10^{-4}$ m/s, $6.38\text{x}10^{-4}$ and $6.91\text{x}10^{-4}$ m/s, $6.40\text{x}10^{-4}$ and $6.98\text{x}10^{-4}$ m/s, respectively, and the negative are $-6.18\text{x}10^{-4}$ and $-6.73\text{x}10^{-4}$ m/s, $-5.92\text{x}10^{-4}$ and $-7.32\text{x}10^{-4}$ m/s, $-6.70\text{x}10^{-4}$ and $-6.81\text{x}10^{-4}$ m/s, respectively. In Figure 13 the numerical and experimental results of horizontal velocity, in m/s, for different positions in the shaft "y" and for a location on the x-axis of 0.04 m are presented. For the non-protuberance system, the component of velocity starts out at zero. Then, the zone of the hydrodynamic boundary layer is subsequently observed where flow is directed horizontally towards the left border. It can be seen that the magnitude of the horizontal velocity increases up to a maximum negative of $-6.40\text{x}10^{-4}$ and $-7.95\text{x}10^{-4}$ m/s, respectively, and from there it

decreases down to a value close to zero; from that point there are small fluctuations of the component of velocity along the central part of the system. The area of the other hydrodynamic boundary layer is observed; now the flow is directed towards the right border. There, the horizontal velocity increases up to a positive maximum of $4.79x10^{-4}$ and $5.26x10^{-4}$ m/s, respectively, and from there again it decreases down to zero. The same behavior is observed for the systems with rectangular, semi-circular, and triangular protuberance but with different values, in this case the maximum negative magnitudes are $-4.91x10^{-4}$ and $-5.28x10^{-4}$ m/s, $-5.73x10^{-4}$ and $-6.78x10^{-4}$ m/s, $-6.01x10^{-4}$ and $-7.52x10^{-4}$ m/s, respectively, and the positive are $3.91x10^{-4}$ and $4.92x10^{-4}$ m/s, $4.22x10^{-4}$ and $5.01x10^{-4}$ m/s, $4.57x10^{-4}$ and $5.13x10^{-4}$ m/s, respectively.

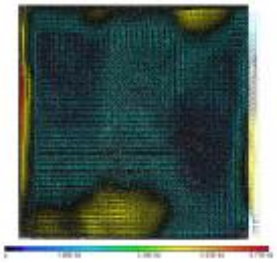

Figure 4. Experimental velocity field, $\vec{V}$, without protuberance.

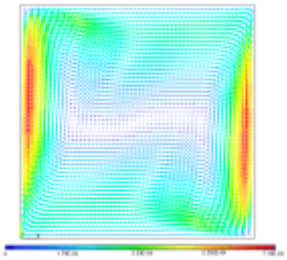

Figure 5. Numerical velocity field, $\vec{V}$, without protuberance.

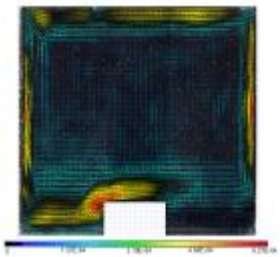

Figure 6. Experimental velocity field, $\vec{V}$, with rectangular protub.

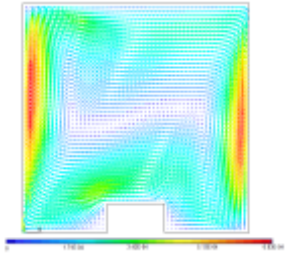

Figure 7. Numerical velocity field, $\vec{V}$, with rectangular protub.

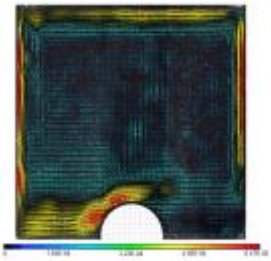

Figure 8. Experimental velocity field, $\vec{V}$, with semi-circular protub.

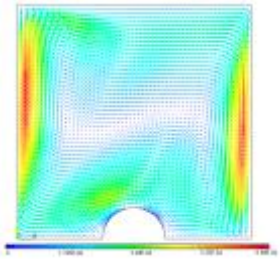

Figure 9. Numerical velocity field, $\vec{V}$, with semi-circular protub.

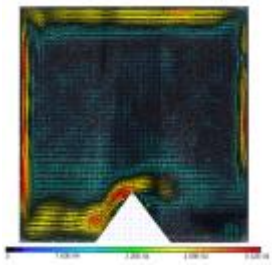

Figure 10. Experimental velocity field, $\vec{V}$, with triangular protuberance.

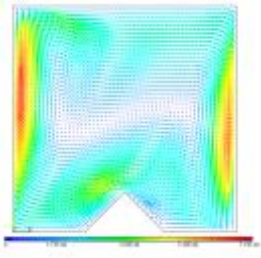

Figure 11. Numerical velocity field, $\vec{V}$, with triangular protuberance.

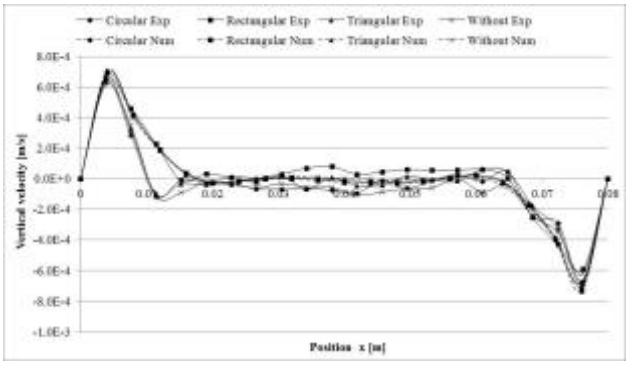

Figure 12. Distribution of horizontal velocity (m/s) for the x=0.04 m position and four protuberances.

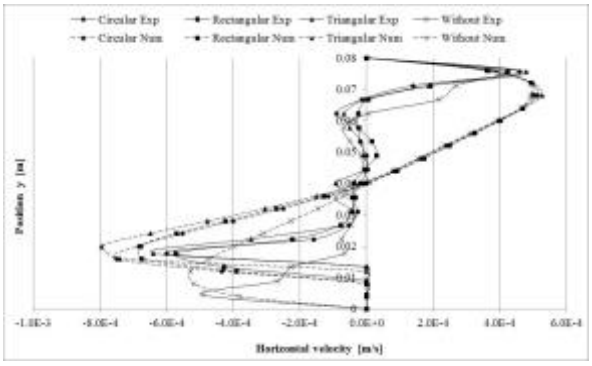

Figure 13 Distribution of vertical velocity (m/s) for the y=0.04 m position and protuberances.

On the other hand, for the calculation of the number of Rayleigh, local Nusselt number and average Nusselt number the equations (7) are used. The average Nusselt numbers are shown in Table 1.

$$Ra = \frac{g\,\beta\,(Tc - Tf)\,H^3\,Pr}{\nu^2} \qquad Nu_{(Y)} = -\left.\frac{\partial\theta}{\partial X}\right|_{X=0} \qquad Nu = \int_0^{\varepsilon}\left(\frac{\partial\theta}{\partial X}\right)_{X=0} dY \qquad (7)$$

Table 1. Average Nusselt's numbers

	Without protub.	Triangular protub.	Semi-circular protub.	Rectangular protub.
Experimental	13.21	12.41	12.16	11.82
Numerical	13.90	13.48	12.64	12.23

The experimental and numerical results showed that both the vertical velocity component and horizontal are diminished by placing the protuberances, finding the highest value in the cavity without protuberance and lowest in the rectangular protuberance. The presence of protuberances generated that in thermal convection occurred a decrease in the average number of Nusselt both for numeric and experimental cases.

7. Conclusions

When comparing the results between systems with rectangular, semi-circular and triangular protuberance, respect to that with no protuberance, it was found that: a) the maximum positive value of the vertical velocity was reduced: 7.12, 3.33, and 3.03%, respectively, for the experimental case and 4.52, 2.26, and 1.27 %, respectively, for the numerical case, b) the maximum positive value of the horizontal velocity was reduced: 18.37, 11.89 and 4.59%, respectively, for the experimental case and 6.46, 4.75 and 2.47%, respectively, for the numerical case, c) the average values of Nusselt number decreased: 10.52, 7.95 and 6.06%, respectively, for the experimental case and 12.01, 9.06 and 3.02%, respectively, for the numerical case. The results can be used to design different equipment heat transfer by natural convection, for example, solar collectors, electric transformers, etc.

8. References

[1] Corvaro F, Paroncini M 2009 An experimental study of natural convection in a differentially heated cavity through a 2D-PIV system *International Journal of Heat and Mass Transfer* Vol. 52 pp 355–365
[2] Corvaro F, Paroncini M, Sotte M 2011 Experimental PIV and interferometric analysis of natural convection in a square enclosure with partially active hot and cold walls *International Journal of Thermal Sciences* 50 pp 1629-1638
[3] Nardini G, Paroncini M 2012 Heat transfer experiment on natural convection in a square cavity with discrete sources *Heat Mass Transfer* 48 pp 1855–1865 DOI 10.1007/s00231-012-1026-6 Springer-Verlag
[4] Kaviany M 1984 Effect of a Protuberance on Thermal Convection in a Square Cavity *Journal of Heat Transfer* Vol. 106 pp 830-834
[5] Qi-Hong Deng 2008 Fluid flow and heat transfer characteristics of natural convection in square cavities due to discrete source–sink pairs *International Journal of Heat and Mass Transfer* 51 pp 5949–5957
[6] Wang X and Pepper D W 2009 Numerical simulation for natural convection in vertical channels *International Journal of Heat and Mass Transfer* 52 pp 4095–4102
[7] Lizardi A, Terres H, López R, Hernández A, Morales J R, Lara A., Zavala C N 2012 Análisis experimental del flujo en cavidades con protuberancias en su interior VII Congreso Bolivariano de Ingeniería Mecánica Cusco Perú
[8] Incropera F P, DeWitt D P 1999 *Fundamentos de Transferencia de Calor* México Prentice Hall
[9] Bejan A 1995 *Convection Heat Transfer* New York Wiley Chap. 4
[10] Moaveni, Saeed 2003 *Finite Element Analysis Theory and Application with ANSYS* 2nd Ed Pearson Education USA